A Study on Ultrasonic Test for Evaluation of Spot Weldability in Automotive Materials

Hyo-Sun Yu* and Byung-Guk Ahn**

(*Received July 14, 1998*)

The evaluation of spot weldability is very important in managing the quality of products and also in increasing the credibility in the automotive manufacturing processes. The purpose of this study is to investigate the applicability of ultrasonic techniques for the evaluation of weldability in spot weldment. Through test results, it is confirmed that the behavior of the average attenuation coefficient(α_{avg}) shows a close relationship with the behavior of tensile-shear strength. The transit time of the ultrasonic pulse echo and nugget size also show a close interrelation. If a larger experimental database with various welding conditions can he collected, then it can he shown that the attenuation coefficient and the transit time of an ultrasonic wave can be effective parameters in the evaluation of spot weldability.

Key Words: Resistance Spot Welding, Spot Weldment, Weldability, Ultrasonic Test, Attenuation Coefficient, Transit time, Tensile-Shear Strength

1. Introduction

Resistance spot welding is an economical method for joining sheet metal components in various manufactured products (Metal Handbook, 7th ed., 1982). This process is especially, widely used for the joining of sheet steel plates in automotive manufacturing processes, because the process is simple, cost-effective, and adaptable to high speed automated production (Orts, 1981; Davidson et al., 1984). A quantitative weldability evaluation test for resistance spot weldments is very important in managing the quality control, and also in increasing the credibility of the automotive manufacturing processes (Sawhill, 1984). Weldability of spot weldments has been mostly evaluated by destructive tests such as peel tests, tensile-shear tests, and cross-tensile tests (Vandenbossche, 1977; Gdeon, 1984,). However, these tests are considered inconvenient for estimating weldability due to their time-consuming nature and the requirement of many specimens. Due to these drawbacks, various trials using the C-scan method and Lamb waves monitoring, etc., are being pursued to overcome these problems (Rokhlin et al., 1985; Rokhlin, 1989; Park Ik Gun, 1994; Young Hyun Nam, 1999).

In this study the possibility for nondestructive evaluation of spot weldability is investigated using ultrasonic techniques. The ultrasonic test is conducted using a local immersion transducer producing a 20MHz longitudinal wave. Further, the tensile-shear test, the macrostructural observation, and the measurement of nugget diameter are also carried out for spot weldments with various welding currents. Finally, the results of these tests are compared and discussed to determine the feasibility of ultrasonic tests for nondestructive evaluation of spot weldability.

* School of Mechanical Engineering, Chonbuk National University, Chonju, Republic of Korea, 561-756, Automobile High Technology Research Institute.

** Nationally Accredited High-Tech. Engineering Center, Chonbuk National University, Chonju, Republic of Korea, 561-756.

2. Experimental Procedure

2.1 Material and specimen

Cold-rolled steel (SPC) plate and galvanized steel (GA45) plate, widely known as automotive

Table 1 The mechanical properties and surface condition of steel plates.

Property / Steel plates	Thickness (mm)	Coating-Zn wt. (g/m^2)	T.S (kg/mm^2)	Y.S (kg/mm^2)	Strain (%)
SPC	1.4		38	20	40
GA45	1.4	45	38	20	40

Table 2 The chemical composition of base metal.

Element / Steel plates	C	Si	Mn	P	S	Ni	Al	Fe
SPC/GA45	0.043	0.019	0.424	0.079	0.007	0.026	0.047	bal.

Table 3 The welding conditions.

Condition / Steel plates	Welding current (kA)	Electrode force (kg)	Squeeze time (cycle)	Welding time (cycle)	Holding time (cycle)
SPC/GA45	5~13	300	30	15	10

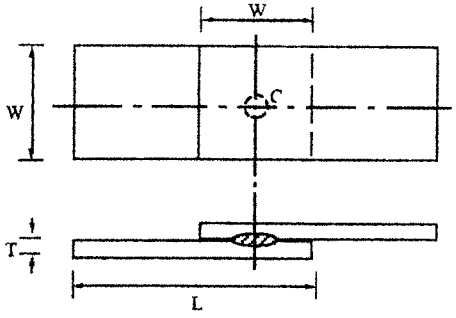

L : 100mm **C : Spot welding center**
T : 1.4mm (Thickness)
W : 30mm

Fig. 1 The schematic diagram of tensile-shear test specimen.

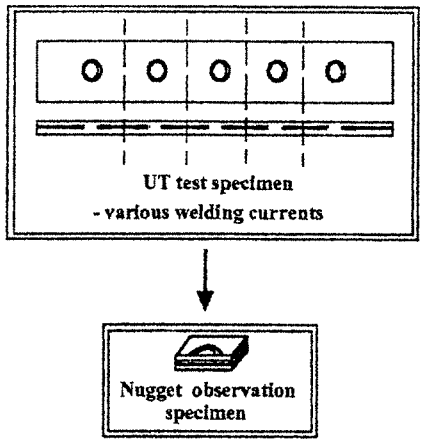

Fig. 2 The schematic diagram of specimens for ultrasonic test and macrostructure observation.

materials, are used in this study. Table 1 shows the mechanical properties and the surface condition of the steel plates used in the terts. The chemical composition of these materials are given in Table 2. To prepare the tensile-shear specimen, two pieces of 100mm×30mm×1.4mm^t steel plates are folded about 30mm, and then one point is welded. Here, the electrode force is controlled to 300kg using a pressure gage, and the flow rate of cooling water is maintained constantly as 6 liter/min. during the welding process. More detailed welding parameters are presented in Table 3. RWMA (Resistance Welder Manufacturer's Association)-class II electrode made of copper base-alumina oxide (Al_2O_3) alloy is used; its diameter and shape are 6mm and dome type, respectively. Two pieces of 150mm×30mm×1.4 mm^t steel plate are folded and 5 points are welded to make the ultrasonic test specimens. After ultrasonic tests, these specimens are centrally machined containing half a nugget to investigate the welded structure and to measure the size of the nugget. Figures 1 and 2 are the schematic diagrams of these specimens and their machining procedures.

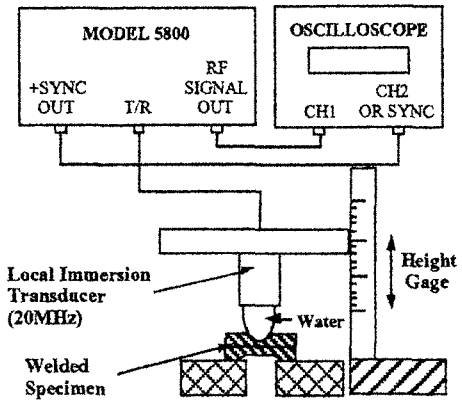

Fig. 3 The schematic diagram of ultrasonic test device.

2.2 Experimental procedures

The tensile-shear test for spot weldment is carried out to evaluate the tensile shear strength using the Instron Tensile Tester with a capacity of 10 tons. The cross head speed is 2mm/min. and the tensile shear strength-displacement curve is plotted using a data acquisition system(DAS). The fracture energy is defined as the area under the tensile-shear strength-displacement curve. The Panametrics 5800 and a local immersion transducer (20MHz-longitudinal wave) are used for the ultrasonic tests. This ultrasonic transducer can especially, be used directly on a spot-welded zone without having a smooth surface due to its captive water column. Further, it is known as a special detector, because the water between the detector and the water column acts as a buffer area. Because the ultrasonic dedecting area closely depends on the diameter of the transducers, the transducer having the diameter 3.2mm which can be applied to all spot welds considering nugget and indentation diameters changeable by spot welding conditions. The attenuation coefficient and the transit time are measured to evaluate the spot weldability under various welding conditions using a digital oscilloscope with a maximum sample rate of 100MS/s. Figures 3 and 4 show the schematic diagrams of the ultrasonic experimental apparatus and the typical shape of an ultrasonic wave, respectively. Samples for the observation of macrostructure and nugget size are polished using emery papers and etched for 30 sec. using 5% nital solution, and then finally observed by an optical microscope.

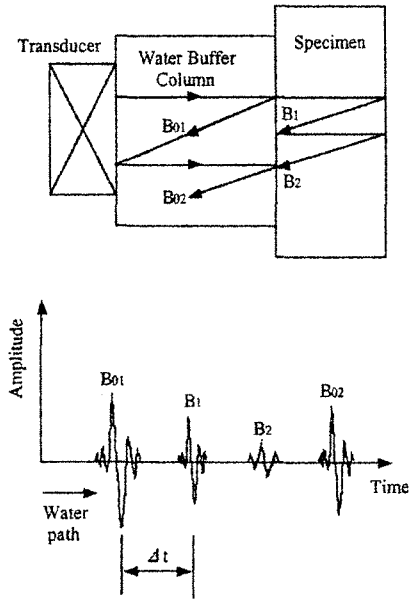

B_{01},B_{02} : First and second echo reflected from buffer-specimen interface

B_1,B_2 : First and second echo reflected from specimen-air imterface(back walf of specimen)

Δt : Transit time

Fig. 4 The schematic diagram of and ultrasonic waveform obtained by local.

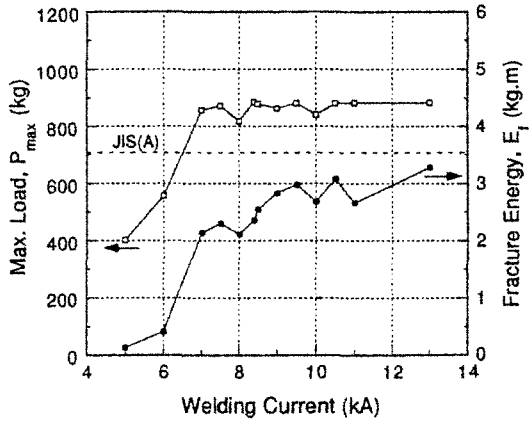

Fig. 5 The effect of welding currents on the tensile-shear strength and the frcture energy for cold-rolled steel plates.

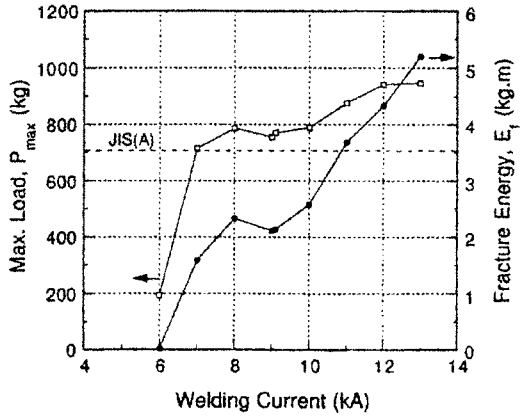

Fig. 6 The effect of welding currents on the shear tensile strength and the fracture energy for galvanized steel plates.

3. Results and Discussion

3.1 Tensile-shear strength behavior with various welding currents

Figure 5 shows the results of maximum load ($P_{max.}$) and fracture energy of the tensile-shear specimen under various welding currents of 5 ~13kA for cold-rolled plates. There is poor tensile-shear strength in the range of low welding currents of 5 and 6kA, but high tensile-shear strength with about 860~880kg is displayed in the range of 7~13kA. Fracture energy is increased as the welding current is increased. From these results, it is noted that the appropriate welding current of cold-rolled steel plates can be considered as 6.4kA when it is compared to the value of the tensile-shear strength (705kg to welding workpiece of thickness 1.4mm) recommended by JIS-A class (JIS Z 3140, 1991).

Figure 6 shows the results of the tensile shear test for galvanized steel plates. The tensile-shear strength is also increased as the welding current is increased. However, the appropriate welding current appears to be about 7kA. Therefore it can be noted that the welding current of galvanized steel plates should be greater than that for cold-rolled plates. In addition, the tensile-shear strength of the galvanized steel plates shows lower values than that of cold-rolled steel plates below 10kA welding current. These facts are attributed to the reduction in welding current density occurred by Zn coating layer with a lower melting temperature.

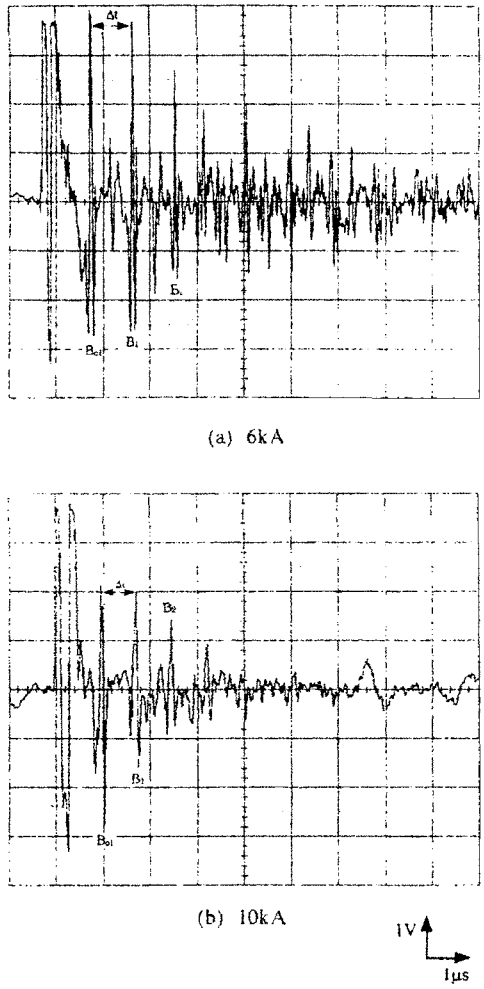

Fig. 7 Typical examples of ultrasonic waveforms for welding currents of 6kA and 10kA in spot weldment of cold-rolled steel plates.

3.2 Average attenuation coefficient behavior with various welding currents

Figures 7 and 8 display typical examples of the first front and back echoes of ultrasonic signals for specimens welded at 6 and 10kA welding currents, respectively. As shown in the figures, the number of multi-reflections in the case of 10kA is smaller than that for 6kA, and further attenuation behavior of ultrasonic signals under high welding currents is also observed.

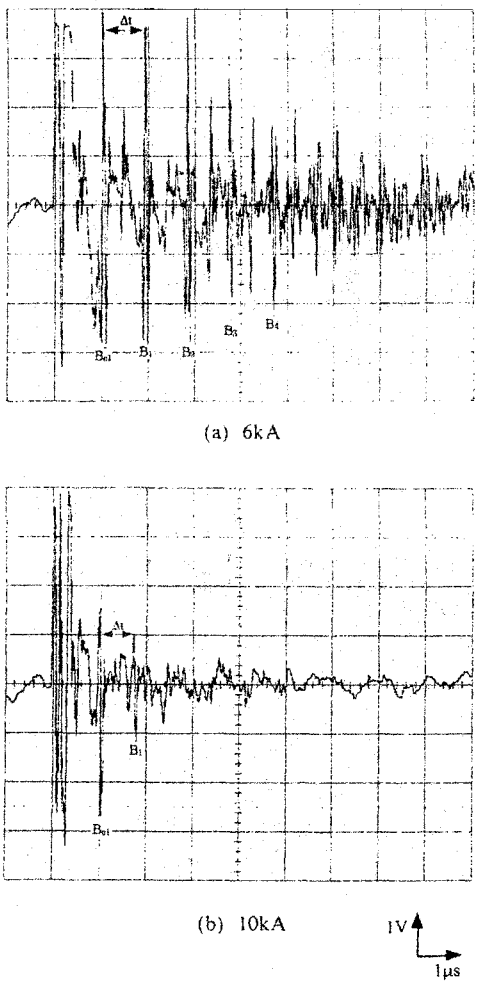

Fig. 8 Typical examples of ultrasonic waveforms for welding currents of 6kA and 10kA in spot weldment of galvanized steel plates.

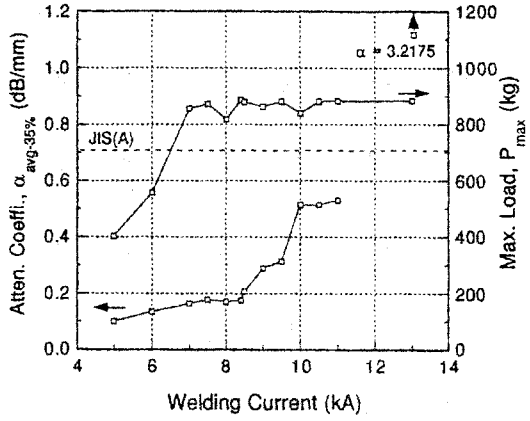

Fig. 9 The effect of welding currents on the attenuation cofficient and the tensile-shear strength for cold-rolled steel plates.

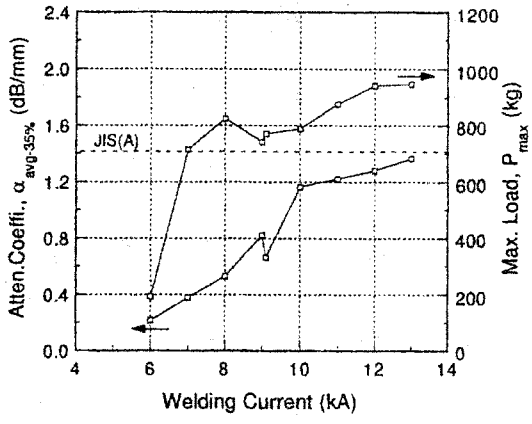

Fig. 10 The effect welding currents on the attenuation coefficient and the shear tensile strength for galvanized stel plates.

Figure 9 shows how the ultrasonic attenuation coefficient and tensile-shear strength are influenced by changes in welding current. Here, the attenuation coefficient(α) is obtained by the Eq. (1).

$$\alpha=\frac{1}{2T}\times\frac{1}{n}\times 20\log_{10}\frac{A_0}{A_n} \qquad (1)$$

where, T=the thickness of specimen, n=the number of echoes on the measured pulse wave, A_0=the amplitude of the initial pulse echo, and A_n=the amplitude of the nth reflection echo. In this study, the average attenuation coefficient (α_{avg}) is calculated using echoes having greater then the 35% amplitude of the initial pulse echo for reproduction of test results. As shown in Fig. 9, the average attenuation coefficient in the low welding current range is about 0.1~0.2dB/mm, indicating almost similar attenuation characteristics. In the range of welding currents above 8.5kA, a high degree of the attenuation behavior is shown. Figure 10 shows the behaviors of the average attenuation coefficient with welding current for galvanized steel plates. The attenuation coefficient increases as the welding current is increased. From this result it can be seen that the average attenuation coefficients corresponding to the available tensile-shear strength recommended

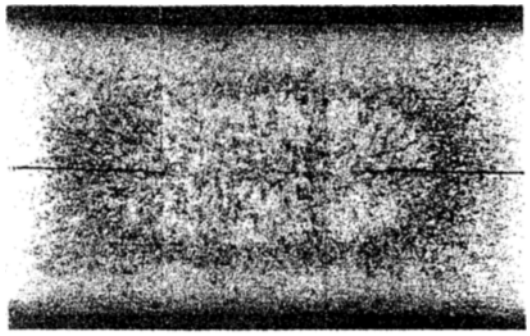

(a) 6kA

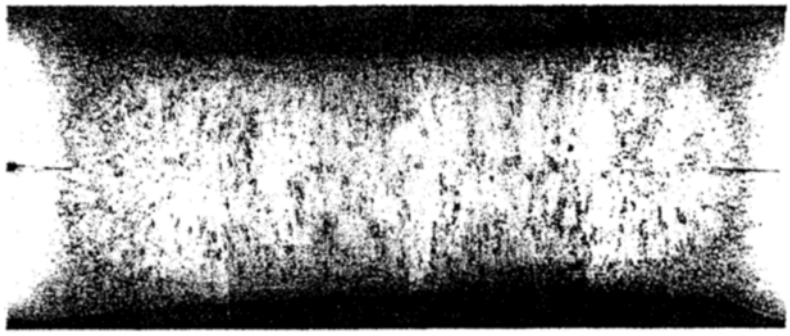

(b) 10kA

Fig. 11 The macroetched photographs of spot weldment for galvanized steel plate

by JIS are considered as 0.15dB/mm for the cold-rolled steel plate and 0.38dB/mm for the galvanized steel plate. Macrostructural observations are made to investigate the causes of changes in ultrasonic attenuation due to variations of welding current. Figure 11 shows the macrostructural photographs of spot weldments welded at 6kA and 10kA for galvanized steel plates. Typical dendritic structures are observed on the weldments and grown by following the direction of heat dissipation. The coarsening of structure in the case of 10kA is more evident than that in 6kA, and also the growth behavior toward the direction of heat dissipation is more effective. This structural change in high welding currents can be mainly attributed to an increase in the attenuation coefficient of the ulatrasonic echo. The galvanized steel plate shows a higher attenuation coefficient than the cold-rolled steel plate for all welding currents. This behavior is caused by the difference in increasing acoustic impedance of microstructures obtained by mixing both Zn coating layers on the surface and base metals for welding.

3.3 Relationship between ultrasonic transit time and nugget size

Figures 12 and 13 show the variations in ultrasonic transit time and nugget size in terms of welding current for both cold-rolled and galvanized steel plates. Further, they also include the

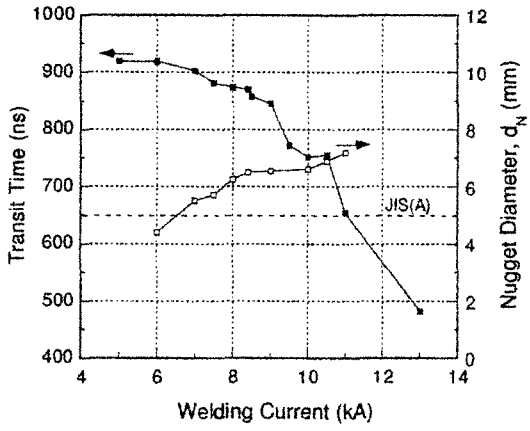

Fig. 12 The effect of welding crrents on the transit time and the nugget diameter for cold-rolled steel plates.

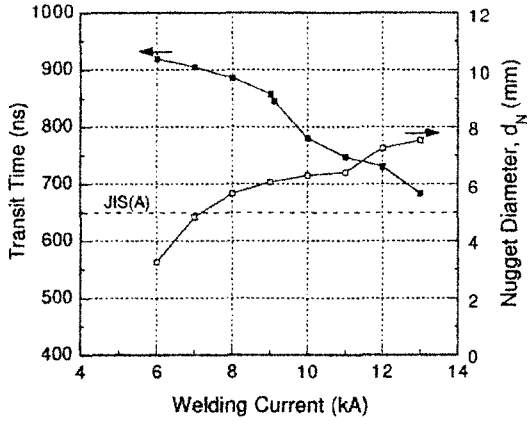

Fig. 13 The effect of welding currents on the transit time and the nugget diameter for galvanized steel plates.

nugget size (5mm to welding workpiece of 1. 4mm thickness) recommended by JIS-A class (JIS Z 3140, 1991). The transit time refers to the duration from the apex of the front-reflected wave (B_{01}) to the one of the back-reflected wave (B_1) in the first pulse echo. As can be seen in the figures, the nugget size increases as welding current is increased. but the transit time is decreased for both steel plates. The increase in nugget size and the decrease in transit time in the galvanized steel plate are more evident than those of the cold rolled steel plates at the same values for increasing weld current. This result is caused by a difference in the current density between the two

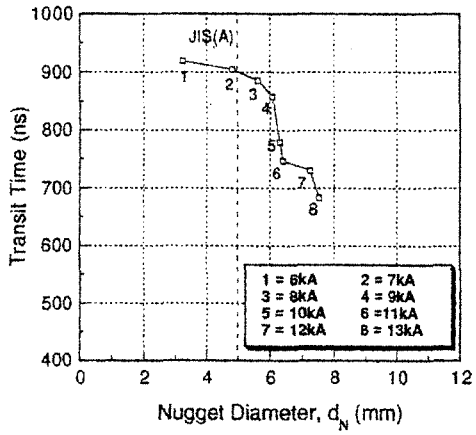

Fig. 14 The relationship between the nugget diameter and the transit time for galvanized steel plates.

steels, which have different surface conditions. Adequate nugget sizes are obtained at welding currents of 6.6kA for the cold rolled plate and 7.2kA for the galvanized steel plate. These values obtained from available nugget diameter of the JIS-A class are a little higher than those values obtained at tensile-shear tests. The ultrasonic transit times corresponding to these weld currents are measured as 908ns for the cold-rolled plate and 900ns for the galvanized steel plate. These results require more analysis with respect to changes in electrode force.

Figure 14 shows the relationship between nugget diameter and transit time for a galvanized steel plate. This figure indicates that two factors are closely interrelated, and that the transit time of the ultrasonic pulse echo can depict the nugget size of spot welds. Generally, the nugget size of spot weldment is considered as an important factor for weldability evaluation, and also the nugget size of the weldment is standardized in automotive spot weld processes. Therefore, it is expected that the transit time parameter can be considered as an important factor in examining the degree of nugget formation.

4. Conclusions

The spot weldability of cold-rolled steel (SPC) and galvanized steel (GA45) plates are evaluated

in terms of the tensile-shear test, the macrostructural observation, the measurement of nugget diameter, and the ultrasonic test. From the test results, it is confirmed that the behavior of the average attenuation coefficient(α_{avg}) shows a close relationship with the behavior of tensile-shear strength. The transit time of an utrasonic pulse echo and nugget size also show a close interrelation. It is expected that this relationship can provide information on the available transit time of ultrasonic waves corresponding to optimum nugget size. The strength of spot weldment and the characteristics of the ultrasonic wave with respect to variations in welding current depend on nugget size and also coarsened dendritic structure through the direction of heat dissipation.

References

Metal Handbook, 7th ed., 1982, "Metals and their Weldability," AWS, Vol. 4.

Orts D. H., 1981, "Fatique Strength of Spot Welded Joints in a HSLA Steel," SAE 810355.

Davidson J. A., Imhofzr E. J., 1984 "The Effect of Tensile Strength on the Fatigue Life of Spot Welded Sheet Steels," SAE 840110.

Sawhiil J. M., 1984, "Spot Weldability Tests for High-Strength Welded Lap Joints," Int. J. Fatigue, Vol. 6, No. 1, pp. 55~57.

Vandenbossche, D. J., 1977, "Ultimate strength and Failure Mode of Spot Welds in High strength Steels," SAE 770214.

Gdeon S. A., 1984, "Metallurgical and Process Variables Affecting the Resistance Spot Weldability of Galvanized Sheet Steels," SAE 840113.

Rokhlin, S. I., Mayhan, R. S. , and Adler, L., 1985, "On-Line Ultrasonic Lamb Wave Monitoring of Spot Welds, Materials Evaluation," Vol. 43, No. 7, pp. 879~883.

Rokhlin, S. I., Meng. S. , and Adler, L. , 1989, "In-Process Ultrasonic Lamb Wave Monitoring of Spot Welds," Materials Evaluation, Vol. 43, No. 7, pp. 897~883.

Park Ik Gun, 1994, "Nondestructive Evaluation of Spot Weld Quality using by Ultrasonic Measurement," Journal of KWS, Vol. 12, No. 3, pp. 109~117.

Young Hyun Nam, 1999, "Directivity Analysis of Ultrasonic Waves on Surface Defects Using a Visualization Method," KSME International Journal, Vol. 13, No. 2, pp. 158~167.

JIS Z 3140, 1991, "Weldability of Spot Weding".